Am J Physiol Renal Physiol. Author manuscript; available in PMC 2016 July 25.

Published in final edited form as:

Am J Physiol Renal Physiol. 2013 March 15; 304(6): F761–F769. doi:10.1152/ajprenal.00263.2012.

Activation of the Ca^{2+}-sensing receptor increases renal claudin-14 expression and urinary Ca^{2+} excretion

Henrik Dimke[1], **Prajakta Desai**[2], **Jelena Borovac**[1], **Alyssa Lau**[2], **Wanling Pan**[1], and **R. Todd Alexander**[1,2]

[1]Department of Physiology and Membrane Protein Disease Research Group, University of Alberta, Edmonton, Alberta, Canada

[2]Department of Pediatrics, University of Alberta, Edmonton, Alberta, Canada

Abstract

Kidney stones are a prevalent clinical condition imposing a large economic burden on the health-care system. Hypercalciuria remains the major risk factor for development of a Ca^{2+}-containing stone. The kidney's ability to alter Ca^{2+} excretion in response to changes in serum Ca^{2+} is in part mediated by the Ca^{2+}-sensing receptor (CaSR). Recent studies revealed renal claudin-14 (Cldn14) expression localized to the thick ascending limb (TAL) and its expression to be regulated via the CaSR. We find that Cldn14 expression is increased by high dietary Ca^{2+} intake and by elevated serum Ca^{2+} levels induced by prolonged 1,25-dihydroxyvitamin D_3 administration. Consistent with this, activation of the CaSR in vivo via administration of the calcimimetic cinacalcet hydrochloride led to a 40-fold increase in Cldn14 mRNA. Moreover, overexpression of Cldn14 in two separate cell culture models decreased paracellular Ca^{2+} flux by preferentially decreasing cation permeability, thereby increasing transepithelial resistance. These data support the existence of a mechanism whereby activation of the CaSR in the TAL increases Cldn14 expression, which in turn blocks the paracellular reabsorption of Ca^{2+}. This molecular mechanism likely facilitates renal Ca^{2+} losses in response to elevated serum Ca^{2+}. Moreover, dys-regulation of the newly described CaSR-Cldn14 axis likely contributes to the development of hypercalciuria and kidney stones.

Keywords

hypercalciuria; CaSR; kidney stones; nephrolithiasis; thick ascending limb

Address for reprint requests and other correspondence: R. T. Alexander, Dept. of Pediatrics, 4-585 Edmonton Clinic Health Academy, 11405-87 Ave., Univ. of Alberta, Edmonton, Alberta, Canada T6G 2R7 (todd2@ualberta.ca).

DISCLOSURES

No conflicts of interest, financial or otherwise, are declared by the authors.

AUTHOR CONTRIBUTIONS

Author contributions: H.D., P.D., and R.T.A. provided conception and design of research; H.D., P.D., J.B., A.L., W.P., and R.T.A. performed experiments; H.D., P.D., J.B., A.L., W.P., and R.T.A. analyzed data; H.D., P.D., J.B., and R.T.A. interpreted results of experiments; H.D., P.D., J.B., and R.T.A. prepared figures; H.D. and R.T.A. drafted manuscript; H.D., P.D., J.B., A.L., W.P., and R.T.A. edited and revised manuscript; H.D., P.D., J.B., A.L., W.P., and R.T.A. approved final version of manuscript.

The prevalence of kidney stones is increasing (33). In some populations, kidney stones have been observed in as many as 12% of men and 5% of women (5). The occurrence of symptomatic stones is strongly dependent on age and race (33), and the recurrence rate is high. Stone disease is expensive to treat due to frequent emergency room visits, hospitalizations, and surgeries. Treatment costs 5 billion dollars annually in the United States alone (30). Moreover, stone disease is directly associated with an increase in the likelihood of adverse renal outcomes, including end-stage renal disease (1).

The greatest risk factor for the development of a Ca^{2+}-containing stone is hypercalciuria (22). Notably, ~80% of stones are calcium (Ca^{2+}) containing (5). Increased urinary Ca^{2+} excretion contributes to Ca^{2+} crystal growth (5). Conversely, a reduction in urinary Ca^{2+} excretion slows stone formation (10, 21). Hypercalciuria may result from disturbed transport of Ca^{2+} in several organs. Increased intestinal absorption or resorption from bone promotes hypercalciuria because renal Ca^{2+} transporters adjust the urinary excretion to maintain serum Ca^{2+} within normal limits (24). Similarly, reduced reabsorption of Ca^{2+} due to disturbances in renal Ca^{2+} reabsorption may also lead to hypercalciuria.

Genetic defects resulting in abnormal renal electrolyte transport can cause hypercalciuria (7). Importantly, mutations in proteins mediating paracellular transport, specifically claudin (Cldn) 16 or Cldn19, cause renal Ca^{2+} wasting (7, 20, 32). These claudins form a cation-permeable paracellular pore in the renal thick ascending limb (TAL) (17, 20, 32). Electrolyte transport in this segment is coupled to the reabsorption of filtered Ca^{2+}. Consequently, ion flux in the TAL is regulated by calciotropic hormones and Ca^{2+} itself (6, 8). Although Ca^{2+}-sensing receptor (CaSR) activation plays a role in this process, the details of downstream signaling remain incompletely elucidated (11).

A large genome-wide association study recently found single nucleotide polymorphisms (SNPs) in human *CLDN14* that strongly associate with kidney stones and lower bone mineral density, inferring a role for Cldn14 in the pathogenesis of idiopathic hypercalciuria (34). Homozygous carriers of the synonymous coding SNP, rs219780[C], had a 1.64-fold increased risk of developing kidney stones. Mutations in the *CLDN14* gene have been identified in two large consanguineous families. Surprisingly, affected individuals have nonsyndromic deafness but do not demonstrate symptoms consistent with Ca^{2+} wasting. Similarly, Cldn14/Cldn11 double knockout mice do not display significantly disturbed urinary Ca^{2+} excretion (9). Thus how Cldn14 contributes to the formation of kidney stones was not clear. Even the renal localization of Cldn14 was a matter of debate (3, 9, 19) until very recently when coimmunolocalization and microdissection experiments demonstrated expression restricted to the TAL (12).

We therefore set out to ascertain the potential role of Cldn14 in regulating renal Ca^{2+} excretion. We found that renal Cldn14 expression is strongly upregulated via activation of the CaSR. In the kidney, Cldn14 mRNA expression remains low until the CaSR is stimulated, dramatically increasing Cldn14 abundance. Moreover, overexpresssion of Cldn14 in a renal epithelial cell model system increases transepithelial resistance and reduces the paracellular flux of cations, including Ca^{2+}. Herein, we clarify two issues. First, our findings corroborate and extend a newly discovered molecular pathway in the TAL that

reduces the renal reabsorptive capacity for Ca^{2+} in response to an increased circulating Ca^{2+} concentration, via CaSR activation (12). Second, these observations suggest that dysregulation of the renal CaSR-Cldn14 pathway could contribute significantly to the development of hypercalciuria, and hence the generation of kidney stones and osteoporosis. Such dysregulation provides a likely molecular explanation as to why SNPs in the CLDN14 gene correlate with kidney stones and lower bone mineral density (34).

MATERIALS AND METHODS

Experimental protocol 1

FVB/N mice (Jackson Laboratories, Bar Harbor, ME) were fed a low (0.01%, TD.95027)-, normal (0.6%, TD.97191)-, or high (2%, TD.00374)-Ca^{2+} diet for either 10 or 21 days (n = 48, 8/group). Diets were custom made by Harlan Laboratories (Madison, WI). Mice were housed in metabolic cages at the end of the experimental period for a 24-h urine collection. On the last day, animals were anesthetized using pentobarbital sodium, and blood was withdrawn by perforating the orbital vessels and *1*) used to measure electrolytes (with a VetScan i-STAT 1 Analyzer, Abaxis, Union City, CA) and *2*) processed into serum. Kidneys were removed and snap frozen in liquid nitrogen. All experimental procedures were approved by the Animal Care and Use Committee for Health Sciences at the University of Alberta (protocol 576).

Experimental protocol 2

FVB/N mice (n = 8/group) were placed on a standard diet with ad libitum access to food and water. 1,25-Dihydroxyvitamin D_3 [1,25$(OH)_2D_3$; Sigma-Aldrich, Oakville, ON] was dissolved in absolute ethanol and diluted to 5% in phosphate-buffered saline. Animals received 1,25$(OH)_2D_3$ (500 pg/g body weight, n = 8) or vehicle (n = 8) by intraperitoneal injections for 5 days. During the last 48 h of the experimental period, mice were placed in metabolic cages. Mice were maintained and processed exactly as described in experimental *protocol 1*.

Experimental protocol 3

FVB/N mice (n = 6/group) were given cinacalcet (Sensipar, Amgen) in food at a dose of 1 mg/g body weight or vehicle. The mice were maintained on a standard diet with ad libitum access to food and water. Animals were kept in regular cages for 2 days and subsequently placed in metabolic cages for the remaining 4 days of the study. The mice were then processed as described in experimental *protocol 1*.

Determination of solutes, creatinine, and hormones

Urinary Ca^{2+} was determined using a colorimetric assay kit (Quantichrom TM Ca^{2+} Assay Kit, BioAssay System, Hayward, CA). Urinary creatinine was measured using a Creatinine Parameter Assay Kit (R&D Systems, Minneapolis, MN). Intact plasma parathyroid hormone (PTH) levels were determined with a mouse PTH ELISA kit (Immutopics International, San Clemente, CA), and serum 1,25$(OH)_2D_3$ concentrations were determined by a γ-radioimmunoassay (RIA) kit (Immunodiagnostic Systems, Fountain Hills, AZ).

Real-time PCR

Total RNA was isolated from kidneys or cells using TRIzol Reagent (Invitrogen, Carlsbad, CA) reverse transcribed into cDNA, which was used to determine gene expression as described in detail previously (25). Primers and probes were made by Integrated DNA Technologies (San Diego, CA). Sequences for primers used to evaluate expression of Cldn14 were as follows: mCldn14: forward primer 5′-TGGCATGAAGTTTGAAATCGG-3′; probe 5′-TGAGAGACAGGGATGAGGAGATGAAGC-3′; reverse primer CG-GGTAGGGTCTGTAGGG. Expression levels were quantified with the ABI Prism 7900 HT Sequence Detection System (Applied Biosystems, Foster City, CA).

Cell culture studies

Opossum kidney (OK) cells were grown and maintained as described previously (25). Monoclonal stable cell lines were generated by transfection of a c-terminal Myc-tagged clone of mouse Cldn14 (NM_001165925.1, OriGene Technologies, Rockville, MD) or the resulting empty vector into OK cells using Fugene 6 (Roche Diagnostics, Laval, Quebec), followed by selection with G418 (Invitrogen). For the evaluation of electrophysical properties, measurements were made in three separate clones isolated from at least three independent transfections of either the empty vector (mock) or Cldn14. Madin-Darby canine kidney (MDCK) cells type II cells expressing mouse Cldn14 under control of the Tet-off system were generated by subcloning Cldn14 with a c-terminal Myc-tag into pTRE2 and then stably transfecting it into MDCK II Tet-Off cells expressing the tetracycline-regulated transactivator (a kind gift of Dr. A. S. Yu). Cells were maintained in Dulbecco's modified Eagle's medium with 10% FBS, 5% penicillin streptomycin glutamine (PSG), 0.1 mg/ml G418, and 0.3 mg/ml hygromycin B. Measurements were made after the cells were grown to confluence (5–7 days) and then in the presence or absence of doxycycline (20 mg/l) for 24 h.

Immunoblotting

Immunoblotting was performed as previously described (25). Briefly, cells were seeded and allowed to reach confluence, then suspended in SDS-PAGE sample buffer (4.6% SDS, 0.02% bromophenol blue, 20% glycerol, 2% 2-ME, 130 mM Tris·HCl, pH 6.8 containing a protease inhibitor cocktail) (Calbio-chem, Gibbstown, NJ). The lysates were subjected to SDS-PAGE and then electroeluted onto nitrocellulose membranes. Mouse primary anti-Myc (9B11) monoclonal antibody (1:1,000, Cell Signaling Technology) was applied overnight at 4°C, followed by incubation with a secondary horseradish peroxidase-coupled secondary antibody (1: 5,000, Santa Cruz Biotechnology, Santa Cruz, CA). Proteins were detected with Western Lightning Plus ECL reagents (PerkinElmer, Boston, MA) and visualized using a Kodak Image Station 440CF (Kodak, Rochester, NY).

Immunocytochemistry

Cells were seeded on glass coverslips and allowed to reach confluence and then fixed using 4% paraformaldehyde (PFA). After being quenched with 5% glycine, the cells were permeabilized with 0.2% Triton X-100. Primary anti-Myc antibody (9B11, Cell Signaling Technology) and rabbit anti-zonula occludens (ZO-1; Invitrogen) were first applied. After washing, secondary DyLight 549 AffiniPure donkey anti-mouse and DyLight 488 AffiniPure

donkey anti-rabbit conjugated antibodies (both from Jackson ImmunoResearch Laboratories) were applied at a dilution of 1:500 for 1 h at room temperature. Specimens were analyzed using a spinning disc confocal microscope (WaveFx, Quorum Technologies, Guelph, Canada).

Ussing chambers

Myc-tagged Cldn14-expressing cells and mock-transfected cells were seeded onto Snapwell inserts (Corning, NY) and grown to confluence. Ussing chamber studies were carried out as described previously (4). Initially, we corrected for the baseline conditions of empty Ussing chambers with *buffer A* (145 mM NaCl, 2 mM $CaCl_2$, 1 mM $MgCl_2$, 10 mM glucose, and 10 mM HEPES, pH 7.4) at 37°C. The Snapwell inserts with confluent OK monolayers were washed three times using *buffer A* and then mounted between the two hemichambers, both of which were filled with 10 ml of *buffer A*. Current clamps were performed using a DVC 1000 I/V Clamp (World Precision Instruments, Sarasota FL), and electrodes containing an agarose bridge with 3 M KCl. Data were acquired as a trace and recorded using PowerLab (ADInstruments, Colorado Springs CO) running Chart 4.0 software. To determine the transepithelial resistance (TER) and permeability properties of the epithelia, a 90-μA current was applied across each monolayer and a dilution potential was induced by replacing *buffer A* in the apical hemichamber with *buffer B* (80 mM NaCl, 130 mM mannitol, 2 mM $CaCl_2$, 1 mM $MgCl_2$, 10 mM glucose, and 10 mM HEPES, pH 7.4). The dilution potential and voltage of each filter were determined following removal of the cells by trypsinization (30 min, at 37°C), and this measurement was subtracted from the values generated by the filter containing cells. Goldman-Hodgkin-Katz and Kimizuka-Koketsu (18) equations were used as described previously (16) to calculate the absolute permeability of Na^+ and Cl^- and to determine the relative permeability of Na^+-to-Cl^- (P_{Na}/P_{Cl}) ratio.

Ca^{2+} flux studies

$^{45}Ca^{2+}$ tracer (PerkinElmer) flux was determined in Ussing chambers with the transepithelial potential difference clamped to 0 mV and equimolar Ca^{2+} in each half of the hemichamber to prevent generating an electrochemical gradient for Ca^{2+} flux across the monolayer. Empty vector (mock)-transfected and cells expressing Myc-tagged Cldn14 were seeded onto Transwell permeable supports (Corning, Corning, NY) and grown for 7 days. $^{45}CaCl_2$ (25 μCi/ml) was applied to the apical hemichamber, and samples were taken sequentially from both the basolateral and apical compartments. Ca^{2+} flux was calculated as the rate of $^{45}Ca^{2+}$ appearance in the basolateral side (cpm/min) divided by the specific activity of radioactivity in the apical side (cpm/mol of Ca^{2+}). Radioactivity of the samples was measured with a LS6500 Multi-Purpose Scintillation Counter (Beckman Coulter).

Statistical analysis

Values are presented as means ± SE. Comparisons between two groups were made using an unpaired Student's *t*-test with Bonferroni correction for multiple comparisons.

RESULTS

High dietary Ca^{2+} intake increases Cldn14 expression

FVB/N mice were placed on a low (0.01%)-, normal (0.6%)-, or high (2%)-Ca^{2+} diet for 10 days. Another group of mice was placed on the same diets for 21 days. The concentration of ionized Ca^{2+} in the blood was not different between groups (Fig. 1*A*). The urinary Ca^{2+}/creatinine (Ca^{2+}/Crea) ratio increased proportionally to the amount of Ca^{2+} in the diet (Fig. 1*B*). There was a significant reduction in serum PTH in mice on high dietary Ca^{2+} for 10 days (Fig. 1*C*). Mice maintained on a low-Ca^{2+} diet had significantly higher serum $1,25(OH)_2D_3$ levels (Fig. 1*D*). Consistent with this, renal expression of 1α-hydroxylase (1α-OHase), the enzyme responsible for the generation of active $1,25(OH)_2D_3$, significantly increased in mice maintained on a low-Ca^{2+} diet (Fig. 1*E*). Conversely, expression of vitamin D-24-hydroxylase (24-OHase), the enzyme that catabolizes active $1,25(OH)_2D_3$ into its inactive form, was significantly increased in animals maintained on a high-Ca^{2+} diet (Fig. 1*F*). Mice maintained on a high-Ca^{2+} diet had a >2.5-fold increase in renal expression of Cldn14 after 10 days and a similar increase after 21 days. We found no difference in renal Cldn14 expression in mice maintained on a low-Ca^{2+} diet vs. a normal diet for either period of time (Fig. 1*G*).

Active $1,25(OH)_2D_3$ increases Cldn14 expression

To determine the potential role of $1,25(OH)_2D_3$ on the expression of Cldn14, animals received daily injections of $1,25(OH)_2D_3$ or vehicle for 5 days. $1,25(OH)_2D_3$ promotes intestinal hyperabsorption and renal transport of Ca^{2+}. Animals injected with $1,25(OH)_2D_3$ developed significantly increased levels of ionized Ca^{2+} in the blood (Fig. 2*A*). The urinary Ca^{2+}/Crea ratio was also elevated, but did not reach statistical significance (Fig. 2*B*). Serum PTH was undetectable in the mice administered $1,25(OH)_2D_3$, and $1,25(OH)_2D_3$ levels were increased (Fig. 2, *C* and *D*). The renal expression of 1α-OHase significantly decreased and 24-OHase was elevated (Fig. 2, *E* and *F*). Renal Cldn14 mRNA expression increased ~10-fold in animals injected with $1,25(OH)_2D_3$ (Fig. 2*G*).

Cldn14 expression is stimulated by calcimimetics in vivo

Renal Cldn14 expression was elevated by a high-Ca^{2+} diet, a condition suppressing PTH and $1,25(OH)_2D_3$. In contrast, administration of $1,25(OH)_2D_3$ increased Cldn14 expression 10-fold while a low-Ca^{2+} diet had no affect on Cldn14 expression, even though it increased $1,25(OH)_2D_3$ levels. Taken together, the data suggest that elevated serum Ca^{2+} is responsible for stimulating renal Cldn14 expression. To test this hypothesis, mice were administered the calcimimetic cinacal-cet hydrochloride (cinacalcet). In these animals, ionized free Ca^{2+} in the blood was significantly reduced, as expected from CaSR hyperactivation (Fig. 3*A*). Consistent with this, animals receiving cinacalcet developed tetany by the end of the experimental period. The urinary Ca^{2+}/Crea ratio was significantly elevated in animals treated with cinacalcet (Fig. 3*B*). PTH levels were undetectable, and $1,25\text{-}(OH)_2D_3$ levels were unaltered (Fig. 3, *C* and *D*). Renal expression of 1α-OHase was decreased, and the expression of 24-OHase was increased (Fig. 3, *E* and *F*). Renal mRNA expression of Cldn14 was increased 40-fold in animals administered cinacalcet (Fig. 3*G*), consistent with the hypothesis that CaSR activation increases renal Cldn14 expression.

Cldn14 forms a preferential cation barrier

We hypothesized that overexpressing Cldn14 would increase TER. As such, we chose to overexpress it in a renal epithelial cell culture model with a very low TER, such as OK cells (4). OK cells were therefore stably transfected with Cldn14 bearing a C-terminal Myc-tag. Dilution potential measurements were performed in confluent monolayers of cells expressing Myc-tagged Cldn14 or cells expressing the empty vector alone (Mock). Consistent with Cldn14 forming a preferential cation barrier, overexpression markedly reduced Na^+ permeability, while the permeability to Cl^- did not decrease significantly (Fig. 4, *A* and *B*). Together, this resulted in a decreased P_{Na}/P_{Cl} ratio (Fig. 4*C*), and a pronounced decrease in the transepithelial flux of Ca^{2+} (Fig. 4*D*). In line with this, overexpression of Cldn14 caused a clear increase in TER (Fig. 4*E*). Immunoblotting of whole cell lysate for Myc detected a single band of ~25 kDa, the predicted size of Cldn14, which was absent in mock-transfected cells (Fig. 4*F*). Expression of Cldn14 mRNA was dramatically increased in the OK cells transfected with the Myc-tagged Cldn14 construct (Fig. 4*G*). Immunofluorescence staining with α-Myc revealed expression of Cldn14 at cell-cell contacts, where it colocalized with ZO-1 (Fig. 4*H*), consistent with localization to the tight junction. In an effort to determine whether Cldn14 expression affected the expression of other claudins, we evaluated the mRNA abundance of claudins known to be expressed in the OK cell line (4). We found that overexpression of Cldn14 did not alter the expression of claudins -1, -4, -9, -12, -15, or -20. However, it induced a threefold increase in Cldn6 expression (Fig. 4*I*).

To verify the functional role of Cldn14 in the tight junction, we also investigated the role of Cldn14 in MDCK II cells using the Tet-off system. The results are listed in Table 1. Overexpression of Cldn14 in this system yielded changes in the P_{Na}/P_{Cl} ratio, P_{Ca}, and TER comparable to those observed in OK cells, suggesting that preferential blockage of cations is a direct effect of increased Cldn14 expression. This is in line with data obtained previously by Ben-Yosef et al. (3).

DISCUSSION

Renal regulation of Ca^{2+} excretion is central to maintaining the serum Ca^{2+} concentration within a tight range. Alterations of this process can cause hypercalciuria, leading to the formation of Ca^{2+}-containing kidney stones (22). The CaSR, which is expressed in the basolateral membrane of the TAL, plays a central role in this process. However, the downstream mechanisms after CaSR activation remain incompletely elucidated. Here, we report that CaSR stimulation prevents paracellular Ca^{2+} flux by increasing renal Cldn14 expression. This is based on the following four observations. *1*) Renal Cldn14 expression is increased with a high-Ca^{2+} diet, while unaltered when dietary Ca^{2+} is low or normal, suggesting that elevated free Ca^{2+} could be the main stimulator of Cldn14 expression. *2*) Increased systemic concentrations of ionized Ca^{2+} observed after chronic $1,25(OH)_2D_3$ administration also leads to marked increases in Cldn14 expression. *3*) Administration of the calcimimetic cinacalcet, which acts on the CaSR to increase its sensitivity to Ca^{2+}, potently induces a 40-fold increase in the abundance of Cldn14. *4*) Overexpression of Cldn14 markedly increases transcellular resistance and decreases paracellular Ca^{2+} flux. Taken

together, these data suggest a mechanism whereby increased circulating Ca^{2+} activates the CaSR, causing increased renal Cldn14 expression. This in turn blocks Ca^{2+}-permeable paracellular pores, preventing the increased amount of filtered Ca^{2+} from being reabsorbed back into the blood. Ultimately, a Ca^{2+} load is excreted, returning circulating Ca^{2+} to normal levels.

Multiple studies have described the renal localization of Cldn14 with conflicting results (3, 9, 19). Recently, a detailed examination of renal Cldn14 expression was performed with *Cldn14*-deficient mice expressing β-galactosidase instead of Cldn14 exon 3. Colocalization studies and quantitative RT-PCR data from dissected nephron segments demonstrated Cldn14 expression in the TAL (12). This nephron segment also expresses the CaSR in its basolateral membrane, permitting the sensing of circulating Ca^{2+} levels (28, 39). We are unable to exclude that a reduction in PTH, which was observed concurrently with increased Cldn14 expression, is responsible for altered levels of expression. However, the major pathway responsible for altered Cldn14 expression is likely via the CaSR, as knockdown of the receptor in vitro ablates the ability of Ca^{2+} to increase Cldn14 expression (12). We found that CaSR activation by different dietary or pharmacological maneuvers markedly upregulated renal Cldn14 mRNA expression. Gong et al. (12) found that increased renal Cldn14 mRNA expression induced by high dietary Ca^{2+} translates into increased renal Cldn14 protein abundance. We expect therefore that a similar relationship is present in our experiments.

Paracellular Ca^{2+} transport across the TAL depends on a lumen-positive transepithelial potential. This gradient appears to be generated by two interdependent mechanisms. The first is the result of asymmetrical secretion of electrolytes, after their influx into TAL epithelial cells. This contributes to a lumen-positive voltage ranging from 5 to 10 mV (14, 15). The second mechanism is the consequence of Na^+ backflux into the lumen of the cortical TAL, a process potentially further increasing the transepithelial potential difference to values as high as 30 mV (13, 16, 23, 29). Backflux of Na^+ occurs via the Cldn16/Cldn19 complex, which forms a cation-permeable pore (17). This same complex likely also permits the paracellular reabsorption of divalent cations down their electrochemical gradient. Mutations in Cldn16 or Cldn19 reduce cation selectivity of this complex and cause familial hypomagnesemia with hypercalciuria and nephrocalcinosis (FHHNC). The pathogenesis of this disease has largely been attributed to a loss of Na^+ backflux, which decreases the lumen-positive driving force (17, 20, 32).

Recently, Gong et al. (12) demonstrated that Cldn14 can interact with Cldn16, but not Cldn19 (12). However, Cldn16 has the ability to bind both claudins. Therefore, the three claudins could potentially exist as a complex. Consistent with this, the coexpression of all three claudins significantly reduced Na^+ permeation relative to overexpression of just Cldn16 and Cldn19 together. Our data are in agreement with this observation. Overexpression of Cldn14 in OK and MDCK II cells dramatically reduces the P_{Na}/P_{Cl} ratio and P_{Ca}, in line with previous reports suggesting that Cldn14 acts as a preferential cation barrier (3, 12). We also observed a threefold increase in the expression of Cldn6, when we overexpressed Cldn14 in OK cells. This contrasts with the ~200-fold increase in Cldn14. As Cldn6 has been shown to decrease P_{Na}, P_{Cl}, and TER, we cannot exclude the possibility that

some of the effect of Cldn14 in OK cells is mediated by increased Cldn6 expression (31). Thus increased Cldn14 expression in the cortical TAL would prevent Ca^{2+} reabsorption by *1*) reducing the permeability of the pore to Ca^{2+} and *2*) blocking backflux of Na^{+}, thereby decreasing the electrochemical gradient driving paracellular Ca^{2+} flux across this segment.

Estimates of the concentration of Ca^{2+} at the bend of the loop of Henle suggest it is almost double (~3 mM) that of superficial proximal puncture sites (~1.8 mM) (2). A high reabsorptive capacity for Ca^{2+} from the TAL is evinced by significantly lower concentrations of Ca^{2+} in fluid obtained from more distal puncture sites (2). Dietary Ca^{2+} loading is expected to increase the distal delivery of Ca^{2+} by several-fold (~3-fold in our dietary Ca^{2+} experiments). During such conditions, modification of the lumen-positive voltage would likely not be enough to prevent significant paracellular reabsorption across the TAL due to the chemical gradient present (lumen to blood). Consequently, altered paracellular P_{Ca} likely contributes significantly to decreased TAL Ca^{2+} reabsorption after activation of the CaSR.

SNPs in the *CLDN14* gene correlate with kidney stone formation, osteopenia, and hypercalciuria. How Cldn14 could cause these abnormalities was not apparent, since a correlation between the risk variants and mRNA expression of Cldn14 in adipose and peripheral blood samples was not observed (34). Very recent data (12) and this study together suggest that significant renal Cldn14 expression is strongly dependent on activation of the CaSR. Low baseline renal expression of Cldn14 explains why patients lacking CLDN14 do not demonstrate evidence of altered Ca^{2+} homeostasis (i.e., stone formation or osteopenia) (38), although detailed physiological characterization may reveal that they are unable to effectively excrete a Ca^{2+} load. Moreover, the urinary excretion of Ca^{2+} in Cldn11/Cldn14 double knockout mice was not altered, providing further evidence that the absence of Cldn14 does not impact renal Ca^{2+} handling under normal dietary conditions (9). A critical experiment confirming a role for Cldn14 in renal Ca^{2+} handling was recently performed (12). *Cldn14*-deficient mice were placed on a high-Ca^{2+} diet and found to have relative hypomagnesiuria and hypocalciuria compared with wild-type controls (12). This response would be expected in the absence of the CaSR-Cldn14 axis, as an increased lumen-to-blood Ca^{2+} concentration gradient would favor increased paracellular Ca^{2+} reabsorption from the TAL.

In some patients, autosomal dominant hypocalcemic hypercalciuria is a result of activating mutations in the *CASR* gene (26, 27). Mild asymptomatic hypocalcemia is generally observed in these patients (26). These mutations cause the half-maximal activity of the receptor to increase (26, 27). More severe activating mutations in the CaSR cause an autosomal dominant form of Bartter's syndrome (27, 35, 37). These individuals have a classic Bartter-like phenotype but differ clinically from individuals with classic Bartter as they have decreased PTH, hypocalcemia, renal Ca^{2+} wasting, and nephrocalcinosis. Discovery of the CaSR-Cldn14 axis provides further insight into these symptoms. Activating mutations in the CaSR would increase Cldn14 expression inappropriately, causing renal Ca^{2+} wasting and nephrocalcinosis. Polymorphisms in the CaSR have also been implicated in idiopathic hypercalciuria (36). As both Cldn14 and the CaSR are now part of a common pathway, association studies may increase their power by grouping CaSR and Cldn14

together. Finally, whether cinacalcet poses a potential risk for the development of kidney stones in patients with primary hyperparathyroidism remains to be established.

In conclusion, our results extend recently published data suggesting that Cldn14 is regulated via a novel CaSR-dependent mechanism (12). Based on these findings, it is likely that Cldn14 plays a key role in the regulation of renal Ca^{2+} excretion. Elegant work from Gong et al. (12) suggests that micro-RNAs binding to the 3′-untranslated region of Cldn14 are regulated by CaSR signaling and in turn alter Cldn14 expression. Whether changes in the micro-RNA recognition sites are responsible for hypercalciuria in humans remains to be determined. Regardless, alterations in the CaSR-Cldn14 axis likely contribute importantly to the development of hypercalciuria and the formation of kidney stones.

Acknowledgments

We thank Drs. J. Casey and S. Frische for insightful comments on the manuscript.

GRANTS

H. Dimke is supported by the Danish Medical Research Council (Forskningsrådet for Sundhed og Sygdom). This work was funded by grants from the Kidney Foundation of Canada and the Canadian Institute of Health Research (To R. T. Alexander). R. T. Alexander is supported by a Clinician Scientist Award from the Canadian Institutes of Health Research and an Alberta Innovates Health Solutions Clinical Investigator Award.

References

1. Alexander RT, Hemmelgarn BR, Wiebe N, Bello A, Morgan C, Samuel S, Klarenbach SW, Curhan GC, Tonelli M. Kidney stones and kidney function loss: a cohort study. BMJ. 2012; 345:e5287. [PubMed: 22936784]
2. Asplin JR, Mandel NS, Coe FL. Evidence of calcium phosphate supersaturation in the loop of Henle. Am J Physiol Renal Fluid Electrolyte Physiol. 1996; 270:F604–F613.
3. Ben-Yosef T, Belyantseva IA, Saunders TL, Hughes ED, Kawamoto K, Van Itallie CM, Beyer LA, Halsey K, Gardner DJ, Wilcox ER, Rasmussen J, Anderson JM, Dolan DF, Forge A, Raphael Y, Camper SA, Friedman TB. Claudin 14 knockout mice, a model for autosomal recessive deafness DFNB29, are deaf due to cochlear hair cell degeneration. Hum Mol Genet. 2003; 12:2049–2061. [PubMed: 12913076]
4. Borovac J, Barker RS, Rievaj J, Rasmussen A, Pan W, Wevrick R, Alexander R. Claudin-4 forms a paracellular barrier, revealing the interdependence of claudin expression in the loose epithelial cell culture model, opossum kidney cells. Am J Physiol Cell Physiol. 2012; 303:C1278–C1291. [PubMed: 23076790]
5. Coe FL, Evan A, Worcester E. Kidney stone disease. J Clin Invest. 2005; 115:2598–2608. [PubMed: 16200192]
6. Desfleurs E, Wittner M, Simeone S, Pajaud S, Moine G, Rajerison R, Di Stefano A. Calcium-sensing receptor: regulation of electrolyte transport in the thick ascending limb of Henle's loop. Kidney Blood Press Res. 1998; 21:401–412. [PubMed: 9933824]
7. Dimke H, Hoenderop JG, Bindels RJ. Hereditary tubular transport disorders: implications for renal handling of Ca^{2+} and Mg^{2+} Clin Sci (Lond). 2010; 118:1–18.
8. Di Stefano A, Wittner M, Nitschke R, Braitsch R, Greger R, Bailly C, Amiel C, Roinel N, de Rouffignac C. Effects of parathyroid hormone and calcitonin on Na^{+}, C^{l-}, K^{+}, Mg^{2+} and Ca^{2+} transport in cortical and medullary thick ascending limbs of mouse kidney. Pflügers Arch. 1990; 417:161–167. [PubMed: 2084613]
9. Elkouby-Naor L, Abassi Z, Lagziel A, Gow A, Ben-Yosef T. Double gene deletion reveals lack of cooperation between claudin 11 and claudin 14 tight junction proteins. Cell Tissue Res. 2008; 333:427–438. [PubMed: 18663477]

10. Ettinger B, Citron JT, Livermore B, Dolman LI. Chlorthalidone reduces calcium oxalate calculous recurrence but magnesium hydroxide does not. J Urol. 1988; 139:679–684. [PubMed: 3280829]
11. Gamba G, Friedman PA. Thick ascending limb: the Na^+:K^+:2Cl^- co-transporter, NKCC2, and the calcium-sensing receptor, CaSR. Pflügers Arch. 2009; 458:61–76. [PubMed: 18982348]
12. Gong Y, Renigunta V, Himmerkus N, Zhang J, Renigunta A, Bleich M, Hou J. Claudin-14 regulates renal Ca^{++} transport in response to CaSR signalling via a novel microRNA pathway. EMBO J. 2012; 31:1999–2012. [PubMed: 22373575]
13. Greger R. Cation selectivity of the isolated perfused cortical thick ascending limb of Henle's loop of rabbit kidney. Pflügers Arch. 1981; 390:30–37. [PubMed: 7195550]
14. Greger R, Schlatter E. Properties of the lumen membrane of the cortical thick ascending limb of Henle's loop of rabbit kidney. Pflügers Arch. 1983; 396:315–324. [PubMed: 6844136]
15. Greger R, Velazquez H. The cortical thick ascending limb and early distal convoluted tubule in the urinary concentrating mechanism. Kidney Int. 1987; 31:590–596. [PubMed: 3550228]
16. Hou J, Paul DL, Goodenough DA. Paracellin-1 and the modulation of ion selectivity of tight junctions. J Cell Sci. 2005; 118:5109–5118. [PubMed: 16234325]
17. Hou J, Renigunta A, Konrad M, Gomes AS, Schneeberger EE, Paul DL, Waldegger S, Goodenough DA. Claudin-16 and claudin-19 interact and form a cation-selective tight junction complex. J Clin Invest. 2008; 118:619–628. [PubMed: 18188451]
18. Kimizuka H, Koketsu K. Ion transport through cell membrane. J Theor Biol. 1964; 6:290–305. [PubMed: 5875308]
19. Kirk A, Campbell S, Bass P, Mason J, Collins J. Differential expression of claudin tight junction proteins in the human cortical nephron. Nephrol Dial Transplant. 2010; 25:2107–2119. [PubMed: 20124215]
20. Konrad M, Schaller A, Seelow D, Pandey AV, Waldegger S, Lesslauer A, Vitzthum H, Suzuki Y, Luk JM, Becker C, Schlingmann KP, Schmid M, Rodriguez-Soriano J, Ariceta G, Cano F, Enriquez R, Juppner H, Bakkaloglu SA, Hediger MA, Gallati S, Neuhauss SC, Nurnberg P, Weber S. Mutations in the tight-junction gene claudin 19 (CLDN19) are associated with renal magnesium wasting, renal failure, and severe ocular involvement. Am J Hum Genet. 2006; 79:949–957. [PubMed: 17033971]
21. Laerum E, Larsen S. Thiazide prophylaxis of urolithiasis. A double-blind study in general practice. Acta Med Scand. 1984; 215:383–389. [PubMed: 6375276]
22. Levy FL, Adams-Huet B, Pak CY. Ambulatory evaluation of nephrolithiasis: an update of a 1980 protocol. Am J Med. 1995; 98:50–59. [PubMed: 7825619]
23. Mandon B, Siga E, Roinel N, de Rouffignac C. Ca^{2+}, Mg^{2+} and K^+ transport in the cortical and medullary thick ascending limb of the rat nephron: influence of transepithelial voltage. Pflügers Arch. 1993; 424:558–560. [PubMed: 8255743]
24. Pak CY, Kaplan R, Bone H, Townsend J, Waters O. A simple test for the diagnosis of absorptive, resorptive and renal hypercalciurias. N Engl J Med. 1975; 292:497–500. [PubMed: 163960]
25. Pan W, Borovac J, Spicer Z, Hoenderop JG, Bindels RJ, Shull GE, Doschak MR, Cordat E, Alexander RT. The epithelial sodium-proton exchanger, Nhe3, is necessary for renal and intestinal calcium (re)absorption. Am J Physiol Renal Physiol. 2012; 302:F943–F956. [PubMed: 21937605]
26. Pearce SH, Williamson C, Kifor O, Bai M, Coulthard MG, Davies M, Lewis-Barned N, McCredie D, Powell H, Kendall-Taylor P, Brown EM, Thakker RV. A familial syndrome of hypocalcemia with hypercalciuria due to mutations in the calcium-sensing receptor. N Engl J Med. 1996; 335:1115–1122. [PubMed: 8813042]
27. Pollak MR, Brown EM, Estep HL, McLaine PN, Kifor O, Park J, Hebert SC, Seidman CE, Seidman JG. Autosomal dominant hypocalcaemia caused by a Ca^{2+}-sensing receptor gene mutation. Nat Genet. 1994; 8:303–307. [PubMed: 7874174]
28. Riccardi D, Lee WS, Lee K, Segre GV, Brown EM, Hebert SC. Localization of the extracellular Ca^{2+}-sensing receptor and PTH/PTHrP receptor in rat kidney. Am J Physiol Renal Fluid Electrolyte Physiol. 1996; 271:F951–F956.
29. Rocha AS, Kokko JP. Sodium chloride and water transport in the medullary thick ascending limb of Henle. Evidence for active chloride transport. J Clin Invest. 1973; 52:612–623. [PubMed: 4685086]

30. Saigal CS, Joyce G, Timilsina AR. Direct and indirect costs of nephrolithiasis in an employed population: opportunity for disease management? Kidney Int. 2005; 68:1808–1814. [PubMed: 16164658]

31. Sas D, Hu M, Moe OW, Baum M. Effect of claudins 6 and 9 on paracellular permeability in MDCK II cells. Am J Physiol Regul Integr Comp Physiol. 2008; 295:R1713–R1719. [PubMed: 18784328]

32. Simon DB, Lu Y, Choate KA, Velazquez H, Al-Sabban E, Praga M, Casari G, Bettinelli A, Colussi G, Rodriguez-Soriano J, McCredie D, Milford D, Sanjad S, Lifton RP. Paracellin-1, a renal tight junction protein required for paracellular Mg^{2+} resorption. Science. 1999; 285:103–106. [PubMed: 10390358]

33. Stamatelou KK, Francis ME, Jones CA, Nyberg LM, Curhan GC. Time trends in reported prevalence of kidney stones in the United States: 1976–1994. Kidney Int. 2003; 63:1817–1823. [PubMed: 12675858]

34. Thorleifsson G, Holm H, Edvardsson V, Walters GB, Styrkarsdottir U, Gudbjartsson DF, Sulem P, Halldorsson BV, de Vegt F, d'Ancona FC, den Heijer M, Franzson L, Christiansen C, Alexandersen P, Rafnar T, Kristjansson K, Sigurdsson G, Kiemeney LA, Bodvarsson M, Indridason OS, Palsson R, Kong A, Thorsteinsdottir U, Stefansson K. Sequence variants in the CLDN14 gene associate with kidney stones and bone mineral density. Nat Genet. 2009; 41:926–930. [PubMed: 19561606]

35. Vargas-Poussou R, Huang C, Hulin P, Houillier P, Jeunemaitre X, Paillard M, Planelles G, Dechaux M, Miller RT, Antignac C. Functional characterization of a calcium-sensing receptor mutation in severe autosomal dominant hypocalcemia with a Bartter-like syndrome. J Am Soc Nephrol. 2002; 13:2259–2266. [PubMed: 12191970]

36. Vezzoli G, Tanini A, Ferrucci L, Soldati L, Bianchin C, Franceschelli F, Malentacchi C, Porfirio B, Adamo D, Terranegra A, Falchetti A, Cusi D, Bianchi G, Brandi ML. Influence of calcium-sensing receptor gene on urinary calcium excretion in stone-forming patients. J Am Soc Nephrol. 2002; 13:2517–2523. [PubMed: 12239240]

37. Watanabe S, Fukumoto S, Chang H, Takeuchi Y, Hasegawa Y, Okazaki R, Chikatsu N, Fujita T. Association between activating mutations of calcium-sensing receptor and Bartter's syndrome. Lancet. 2002; 360:692–694. [PubMed: 12241879]

38. Wilcox ER, Burton QL, Naz S, Riazuddin S, Smith TN, Ploplis B, Belyantseva I, Ben-Yosef T, Liburd NA, Morell RJ, Kachar B, Wu DK, Griffith AJ, Riazuddin S, Friedman TB. Mutations in the gene encoding tight junction claudin-14 cause autosomal recessive deafness DFNB29. Cell. 2001; 104:165–172. [PubMed: 11163249]

39. Yang T, Hassan S, Huang YG, Smart AM, Briggs JP, Schnermann JB. Expression of PTHrP, PTH/PTHrP receptor, and Ca^{2+}-sensing receptor mRNAs along the rat nephron. Am J Physiol Renal Physiol. 1997; 272:F751–F758.

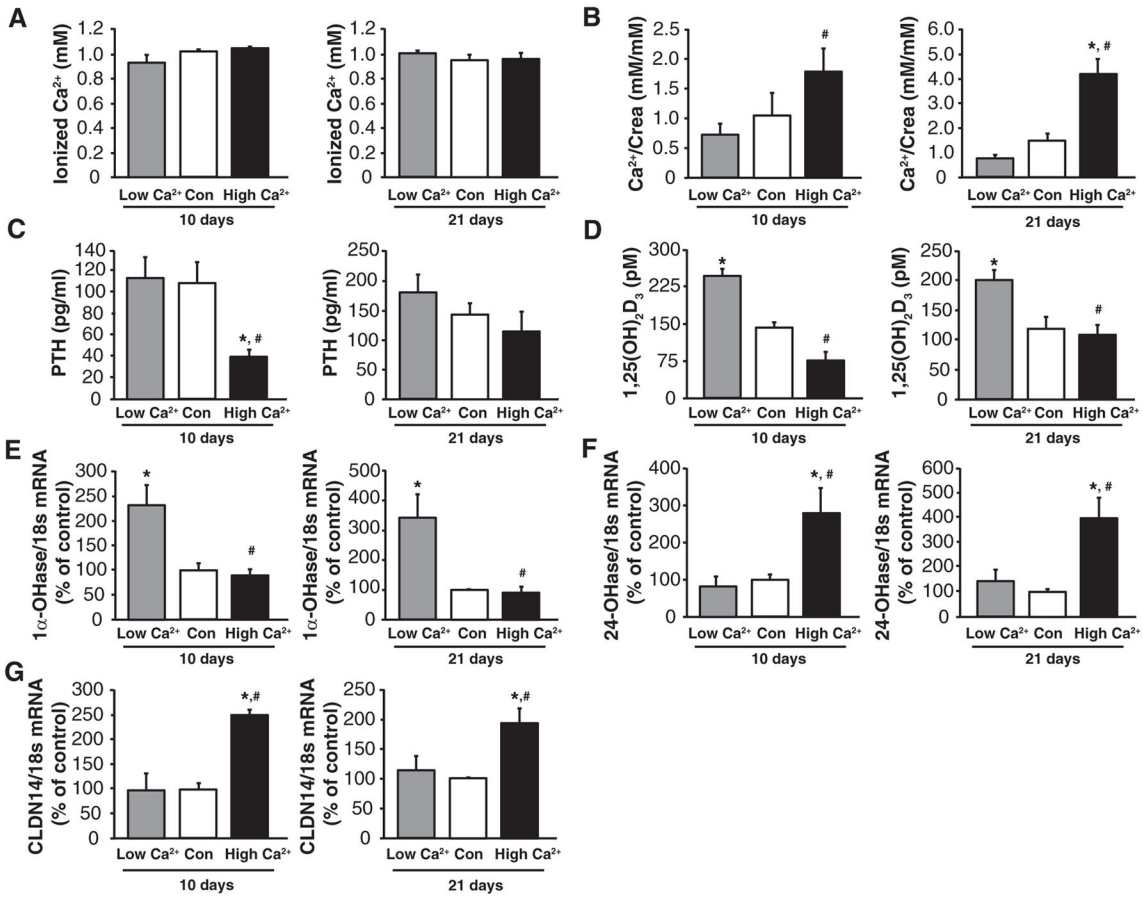

Fig. 1.

High dietary Ca^{2+} increases claudin (Cldn) 14 expression. *A* and *B*: serum ionized Ca^{2+} (*A*) and urinary Ca^{2+}/creatinine (Crea) ratio (*B*) in mice receiving a diet containing low (0.01%), normal (0.6%), or high (2%) Ca^{2+} content for either 10 or 21 days. Also shown are parathyroid hormone (PTH; *C*) and 1,25-dihydroxyvitamin D_3 [$1,25(OH)_2D_3$; *D*] levels measured in serum, renal mRNA expression of 1α-hydroxylase (1α-OHase; *E*) and D-24-hydroxylase (24-OHase; *F*) in mice on different dietary amounts of Ca^{2+}, and renal Cldn14 mRNA expression (*G*). Values are means ± SE. *$P < 0.05$ relative to animals maintained on the control diet. #$P < 0.05$ relative to animals maintained on low dietary Ca^{2+}.

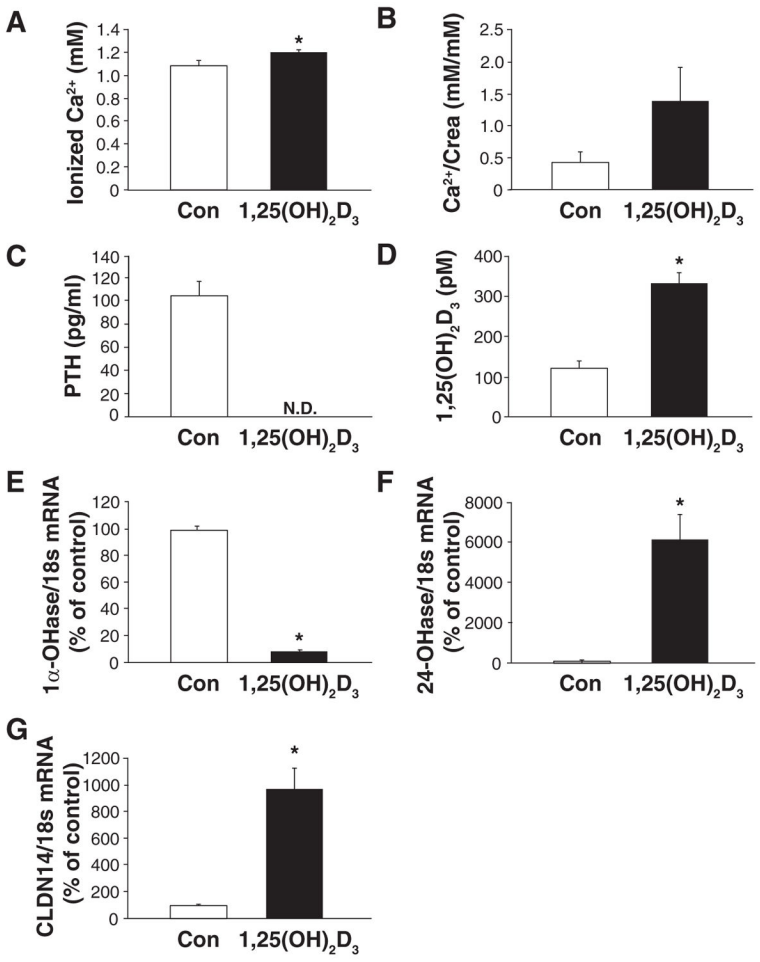

Fig. 2.

$1,25(OH)_2D_3$ administration increases renal Cldn14 abundance. *A* and *B*: serum ionized Ca^{2+} (*A*) and urinary Ca^{2+}/Crea ratio (*B*) in mice injected ip with $1,25(OH)_2D_3$ for 5 days. Also shown are serum levels of PTH (*C*) and $1,25(OH)_2D_3$ (*D*), renal mRNA expression of 1α-OHase (*E*) and 24-OHase (*F*) in animals treated with $1,25(OH)_2D_3$ or vehicle (Con), and expression of renal Cldn14 mRNA in response to chronic administration of $1,25(OH)_2D_3$ (*G*). Values are means ± SE. PTH was not detectable (ND) in mice administered $1,25(OH)_2D_3$. $*P < 0.05$ relative to animals receiving vehicle injection (control).

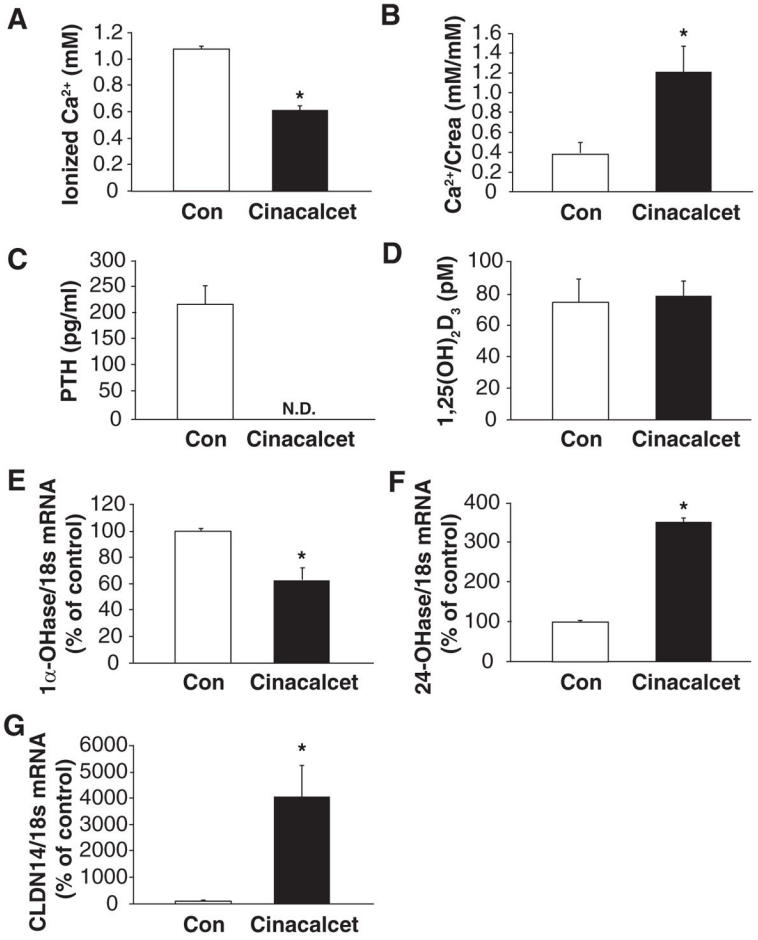

Fig. 3.

Cinacalcet increases the renal expression of Cldn14 serum ionized Ca^{2+} (*A*) and urinary Ca^{2+}/Crea ratio (*B*) in mice receiving either vehicle (Con) or cinacalcet in their diet. Also shown are PTH (*C*) and $1,25(OH)_2D_3$ levels (*D*) from serum of vehicle (Con) or cinacalcet-treated mice, renal mRNA expression of 1α-OHase (*E*) and 24-OHase (*F*), and renal Cldn14 mRNA abundance (*G*) after chronic administration of cinacalcet or vehicle (Con). Values are means ± SE. $*P < 0.05$ relative to animals treated with vehicle.

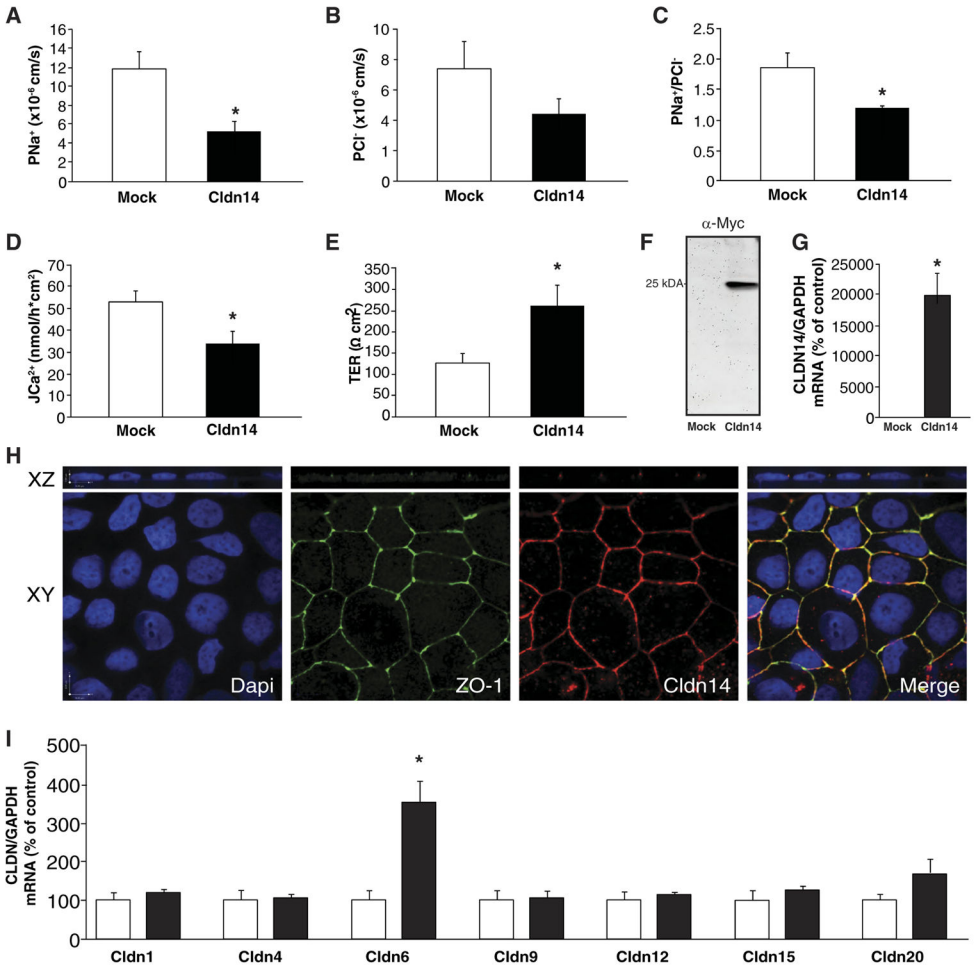

Fig. 4.

Cldn14 increases transepithelial resistance by blocking paracellular ion permeation. *A* and *B*: permeability measurements for Na^+ and Cl^- across confluent monolayers of opossum kidney (OK) cells expressing Myc-tagged Cldn14 (black bars) or empty vector (Mock; white bars). *C*: Na-to-Cl permeability ratio (P_{Na}/P_{Cl}) of OK cells stably expressing Myc-tagged Cldn14 or empty vector. *D*: $^{45}Ca^{2+}$ flux across confluent monolayers of OK cells expressing Cldn14 or empty vector. *E*: transepithelial resistance (TER) of confluent monolayers of OK cells stably transfected with Myc-tagged Cldn14 or control. *F*: immunoblot of whole cell lysate from OK cells stably expressing Myc-tagged Cldn14 or mock-transfected cells. *G*: mRNA expression of mouse Cldn14 in OK cells stably transfected with mock or Cldn14. *H*: representative confocal images through *XZ* and *XY* planes of OK cells expressing Myc-tagged Cldn14, immunostained for zonula occludens (ZO)-1, Myc (Cldn14), and 4,6-diamidino-2-phenylindole (DAPI). Scale bars represent 8 μM in the *XY* planes and 1 μM in the *Z*-axis. *I*: mRNA abundance of claudins known to be endogenously expressed in OK cells in stable clones expressing either Myc-tagged Cldn14 or mock. Values are means ± SE. $*P < 0.05$ relative to control transfected cells; $n \geq 3$ independent stable cell lines.

Table 1

MDCK type II cells expressing Cldn14 controlled by the Tet-Off system

Measurement	+Dox (Control)	−Dox (Cldn14 Expressed)
TER, Ω^{*} cm^2	65 ± 8	102 ± 14*
P_{Na}, 10^{-5} cm/s	2.35 ± 0.4	1.27 ± 0.1*
P_{Cl}, 10^{-5} cm/s	1.20 ± 0.2	0.88 ± 0.2
P_{Na}/P_{Cl}	2.18 ± 0.4	1.50 ± 0.1*
P_{Ca}	47.2. ± 1.7	31.8 ± 3.2*

Values are means ± SE. MDCK, Madin-Darby canine kidney; Cldn, claudin; Dox, doxycycline; TER, transepithelial resistance; *P*, permeability.

$^{*}P < 0.05$; $n = 3$/condition.